

Bulk Compton motion in the luminous quasar 4C04.42?

A. De Rosa^{1*}, L. Bassani², P. Ubertini¹, A. Malizia², A. J. Dean³

¹INAF/IASF-Roma, via del Fosso del Cavaliere 100, I-00133 Rome, Italy

²INAF/IASF-Bologna, via Gobetti 101, I-40129 Bologna, Italy

³School of Physics and Astronomy, University of Southampton Highfield, Southampton, United Kingdom

10 November 2018

ABSTRACT

We present the broadband analysis of the powerful quasar 4C04.42 ($z=0.965$) observed by *XMM-Newton* and *INTEGRAL*. The 0.2–200 keV spectrum is well reproduced with a hard power-law component ($\Gamma \sim 1.2$), augmented by a soft component below 2 keV (observer frame), which is described by a thermal blackbody with temperature $kT \simeq 0.15$ keV. Alternatively, a broken power-law with $E_{break}=2$ keV and $\Delta\Gamma=0.4$ can equally well describe the data. Using archival data we compile the not-simultaneous Spectral Energy Distribution of the source from radio to gamma-ray frequencies. The SED shows two main components: the low frequency one produced by Synchrotron radiation from the electrons moving in the jet and the high energy one produced through external Compton scattering of the electrons with the photon field of the Broad Line Region. Within this scenario the excess emission in the soft-X ray band can be interpreted as due to Bulk Compton radiation of cold electrons. However, some other processes, briefly discussed in the text, can also reproduce the observed bump.

Key words: Galaxies: active - Galaxies: individual: 4C04.42 - quasars: general - X-rays: galaxies

1 INTRODUCTION

Blazars are the most powerful objects in the observable Universe, and are capable to emit from radio frequencies up to the extreme gamma-ray. In the X-ray energy range, harder spectra are associated with the highest luminosity objects (Fossati et al. 1998), and Flat Spectrum Radio Quasars (FSRQ) are the most luminous class of Blazars. The Spectral Energy Distribution (SED) of FSRQ exhibits two main peaks (one between the IR and soft X-ray frequencies and the other in the gamma-ray regime), disclosing the presence of two main components: it is widely believed that the low energy one is due to the Synchrotron radiation of relativistic electrons in a jet, while the high energy one is due to Inverse Compton scattering (IC) of the same electrons with a photon field (Ghisellini et al. 1998). It is also believed that in FSRQ the IC is due to Compton scattering of photons external to the jet (external Compton radiation EC), probably produced in the accretion disk and reprocessed by the Broad Line Region (BLR) and/or the dusty torus (Dermer & Schlickeiser 1993; Wagner et al. 1995). Other competitive processes, like the IC from photons produced by Synchrotron (Synchrotron Self-Compton radiation, SSC) can contribute to the high energy component (Maraschi et al. 1992). The investigation of these extreme objects in the X-ray band is important mainly because they emit most of their bolometric luminosity in this energy range (Elvis et al. 1994) and because the fast variability indicates that this radiation is produced very close to the

central black-hole. Observations have demonstrated that radio-loud QSOs are more powerful X-ray emitters than radio-quiet counterparts or RQQs (Page et al. 2005) and, therefore, more easily observable. Various authors (Reeves & Turner 2000; Piconcelli et al. 2005) have demonstrated that radio-loud QSOs exhibit a flatter intrinsic spectral shape ($\Gamma \sim 1.6$) than RQQs ($\Gamma \sim 1.9$); this harder X-ray emission is thought to be Synchrotron or IC emission from the relativistic radio jet, rather than from the accretion disk.

A deficit of photons in the soft X-ray band ($E < 2$ keV observer frame) of several high and low- z QSOs has been observed in the past by *ASCA* (Fabian et al. 1998; Fiore et al. 1998), and recently confirmed through *XMM-Newton*, *Chandra* and *Swift* observations (Bassani et al. 2007; Yuan et al. 2006; Sambruna et al. 2007). The origin of this feature is not yet clear. Possible hypotheses are an intrinsic cold/ionized absorption or an intrinsic break of the continuum. When associated with absorption a clear trend of N_H vs z has been measured, indicating a cosmic evolution effect, which seems to be strongest at redshifts around 2 (Yuan et al. 2006). However, excess emission at similar low energies has also been observed, but only in a few sources (Kataoka et al. 2007; Sambruna et al. 2006). The origin of this behaviour is still unclear, even if several scenarios have been proposed and explored, like Bulk Comptonization (Celotti et al. 2007), increasing contribution of the SSC component, (Kataoka et al. 2007), and reflection from the accretion disk (Sambruna et al. 2006). So far these two spectral features (excess or deficit of soft X-ray photons), have been interpreted as due to different emission processes. However, very recently, Celotti et al. (2007) modelled the soft X-ray flattening observed in the quasar

* E-mail: alessandra.derosa@iasf-roma.inaf.it

Table 1. Journal of the *XMM-Newton* and *INTEGRAL* observation of 4C04.42

Instrument	Date	Exp Time (s)	RA, DEC (J2000) (h m s, °'")	Counts/s (s ⁻¹)
<i>XMM-Newton</i> -MOS1 (thin filter)	2006/07/12	11515	12 22 22.50,+04 13 16.0	*0.173±0.005
<i>XMM-Newton</i> -MOS2 (thin filter)	2006/07/12	11527	12 22 22.50,+04 13 16.0	*0.213±0.006
<i>XMM-Newton</i> -pn (thin filter)	2006/07/12	8842	12 22 22.50,+04 13 16.0	†0.83±0.01
<i>INTEGRAL</i> -isgri	-	100000	12 22 26.88, +04 15 21.6	°0.12±0.02

* In 0.5-10 keV. † In 0.3-12 keV. In ° In 20-100 keV for IBIS/ISGRI.

BG B1428-4217, via bulk Comptonization process. Clearly more sources need to be observed in order to improve the statistics and study their physical properties in more detail.

4C04.42 is a FSRQ, with radio loudness parameter $R=S_{5\text{GHz}}/S_{4400\text{\AA}} \sim 1000$ (Kellermann et al. 1989). It was detected above 20 keV by *INTEGRAL* (Bird et al. 2007) with a flux of $(7.6 \pm 1.5) \times 10^{-12}$ erg cm⁻² s⁻¹ and $(18.8 \pm 2.8) \times 10^{-12}$ erg cm⁻² s⁻¹ in 20-40 keV and 40-100 keV bands respectively. It was later observed by *XMM-Newton* for ~ 10 ks. In this letter we present the broadband analysis of 4C04.42 in 0.2-200 keV, for the first time, through non simultaneous *XMM-Newton* and *INTEGRAL* data and provide strong evidence for soft excess emission below 2 keV. In Sect. 2 we present the observations and data reduction, in Sect. 3 we describe the detailed spectral analysis, while the discussion is reported in Sect. 4. We draw our conclusions in Sect. 5. Throughout this paper we adopt a luminosity distance of $d_L = 6358$ Mpc for 4C04.42 ($z = 0.965$), derived for a Λ CDM cosmology with $\Omega_m = 0.27$, $\Omega_\Lambda = 0.73$ and $H_0 = 71$ km s⁻¹ Mpc⁻¹.

2 OBSERVATIONS AND DATA REDUCTION

2.1 *XMM-Newton*

XMM-Newton observed 4C04.42 in July 2006 and details of this observation are given in Table 1. EPIC data reduction was performed with version 7.0 of the SAS software, employing the most updated calibration files available at the time of the data reduction (2007 May). Patterns 0 to 12 (4) were employed in the extraction of the MOS (pn) scientific products. EPIC-pn and EPIC-MOS spectra for the source and background were extracted from a circular region of 30 arcsec radius around the source and from a source-free region respectively. Spectra were rebinned to have at least 20 counts in each spectral channel. Spectral fits were performed simultaneously with MOS1, MOS2 (0.3–9 keV) and pn (0.8-10 keV). The results obtained fitting the data of MOS1/MOS2 and pn separately will also be discussed in the Sect. 3.

2.2 *INTEGRAL*

INTEGRAL-IBIS (Ubertini et al. 2003) data have been reduced following the same procedure used for the survey work and described in Bird et al. (2007). The source was detected with a significance of $\sim 8\sigma$. First IBIS/ISGRI images for each available pointing were generated in 13 energy bands using the ISDC offline scientific analysis software OSA version 5.1. Count rates at the source position were extracted from individual images in order to provide light curves in the various energy bands sampled. Since the light curves did not show any sign of variability or flaring activity, average fluxes were then extracted in each band and combined to produce the source spectrum. We tested the reliability of this spectral extraction method by comparing the Crab spectrum obtained in this way with the one extracted using the standard spectral analysis.

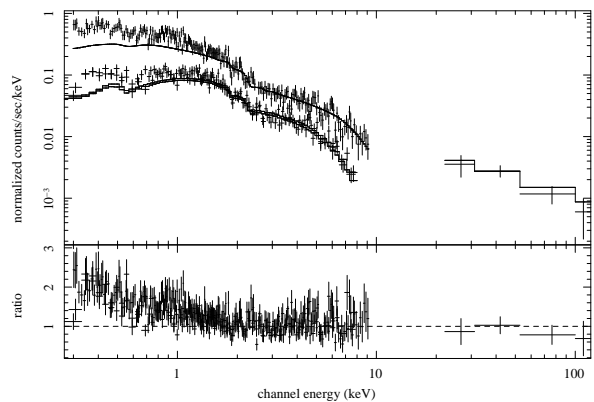


Figure 1. Continuum power-law fit to the energy band above 2 keV (observer frame) extrapolated over the low energy range. *Top curve*: pn data, *bottom curve*: MOS.

3 *XMM-Newton* AND *INTEGRAL* DATA ANALYSIS

We performed spectral analysis with XSPEC v11.3. Errors correspond to 90 per cent confidence level for one interesting parameter ($\Delta\chi^2=2.7$). All parameters values in the text and tables refer to those measured in the observer frame, if not otherwise specified. To reproduce the intrinsic continuum of 4C04.42 we fitted *XMM-Newton* and *INTEGRAL* data over the 2-150 keV band with an absorbed power-law and obtain a good fit with photon index $\Gamma=1.21^{+0.06}_{-0.06}$ and the column density fixed to the Galactic value ($N_H=1.69 \times 10^{20}$ cm⁻²). This absorbed power-law, extrapolated to the 0.3–2 keV band, fails to reproduce the observed spectrum (see Figure 1, and first line in Table 2), giving a $\chi^2/dof=428/366$. Major residuals are seen at low energies, strongly suggesting the presence of excess emission below 2 keV. To fit more accurately the combined *XMM-Newton* and *INTEGRAL* spectrum, and to fully account for the extra low energies component, we tried a range of different models. In Table 2 we report the best fit parameters for each of them. Fitting the excess with a thermal black-body model in addition to the absorbed power-law we obtain a good result ($\chi^2/dof=383/364$), with kT_{BB} around 0.15 keV. A multiple black-body component (diskbb in XSPEC) reproduces the excess even better than the single temperature black-body ($\chi^2/dof=373/364$). We also tested the possibility that the observed behaviour is due to a break in the intrinsic continuum. We substituted the primary power-law with a broken power-law without including any other emission component at low energies. Following this representation we found that, at energies below $E_{break} \sim 2$ keV, the continuum photon index is steeper than above E_{break} , with $\Delta\Gamma \sim 0.4$ (see Table 2). In this case we find a good fit, with $\Delta\chi^2=8$ with respect to the multiple blackbody model. However, the null hypothesis probability in this case, increases by only ~ 10 per cent with respect

Table 2. Best-fit parameters of the different models we used to reproduce the combined broadband (0.2–200 keV) *XMM-Newton* and *INTEGRAL* data.

$^1C_{integral}$	χ^2/dof	$^2P_{null}$	Γ	$F^{obs}(0.1-2 \text{ keV})$ ($10^{-12} \text{ erg cm}^{-2} \text{ s}^{-1}$)	$F^{obs}(2-10 \text{ keV})$ ($10^{-12} \text{ erg cm}^{-2} \text{ s}^{-1}$)	$F^{obs}(20-100 \text{ keV})$ ($10^{-12} \text{ erg cm}^{-2} \text{ s}^{-1}$)	param
constant phabs zpowerlw							
1 frozen	428/366	0.01	$1.44^{+0.03}_{-0.03}$	1.0	2.2	8.2	–
1.9 ± 0.5	419/365	0.03	$1.44^{+0.03}_{-0.03}$	1.0	2.2	8.0	–
constant phabs zpowerlw zbb							
1 frozen	383/364	0.232	$1.28^{+0.02}_{-0.04}$	0.98	2.5	13	$0.15^{+0.02}_{-0.02}$
$1.2^{+0.3}_{-0.3}$	383/363	0.229	$1.30^{+0.04}_{-0.03}$	0.99	2.5	13.	$0.15^{+0.02}_{-0.02}$
constant phabs zpowerlw diskbb							
1 frozen	373/364	0.363	$1.22^{+0.06}_{-0.06}$	1.0	2.5	15	$0.25^{+0.04}_{-0.04}$
$0.97^{+0.04}_{-0.03}$	373/363	0.349	$1.22^{+0.07}_{-0.08}$	1	2.5	15	$0.26^{+0.04}_{-0.04}$
constant phabs brokenpowerlw							
1 frozen	365/364	0.476	$1.58^{+0.05}_{-0.04}$	1.0	2.5	16.	$2.1^{+0.4}_{-0.3}$
$0.9^{+0.3}_{-0.3}$	364/363	0.470	$1.19^{+0.07}_{-0.05}$ $1.59^{+0.05}_{-0.05}$ $1.17^{+0.09}_{-0.10}$	1.0	2.6	17	$2.2^{+0.4}_{-0.4}$
constant phabs zbb pexrav							
1 frozen	382/363	0.233	$1.33^{+0.09}_{-0.08}$	1.0	2.6	14	$0.25^{+0.42}_{-0.24}$
$1.1^{+0.4}_{-0.3}$	382/362	0.224	$1.33^{+0.07}_{-0.08}$	1.0	2.5	14	<0.6

¹ Cross-calibration constant *INTEGRAL*-isgri/*XMM-Newton*-MOS1; ² Null hypothesis probability. ³ in keV.

to the diskbb model, suggesting that strong statistical evidence does not exist for broken power-law to be preferred over the thermal one. The luminosity of the black-body component in the 0.1–3 keV band is $L_{BBbody} \sim 10^{45} \text{ erg s}^{-1}$. Testing for the presence of a Compton reflection component, using the model *pexrav* in XSPEC (Magdziarz & Zdziarski 1995), we find only an upper limit for the relative reflection ($R = \Omega/2\pi < 0.6$). No evidence for an iron line is found in the data. Properly redshifted, we included a narrow gaussian line at the energy of cold Fe, obtaining an upper limit for the line intensity $I_{Fe} \leq 10^{-6} \text{ ph cm}^{-2} \text{ s}^{-1}$ (i.e. $EW_{Fe} \leq 15 \text{ eV}$). We stress here that the estimated value of the Compton reflection fraction R is strongly dependent on the value of the cross-calibration constant $C_{integral}$ between the soft gamma (*INTEGRAL*) and X-ray (*XMM-Newton*) data. In this respect, we note that Kirsch and collaborators (2005) analysed the Crab spectrum observed with different instruments and concluded that at 20 keV the *XMM-Newton/INTEGRAL* cross-calibration was close to 1 (within few per cent). However we also checked this assumption a posteriori repeating all the spectral fits, leaving $C_{integral}$ free to vary. The best fit parameters are also included in Table 2. The value of $C_{integral}$ is always well constrained around one and the main results of the analysis we have presented do not change leaving $C_{integral}$ free to vary. The same outcome is found if the combined MOS1/MOS2 and pn data are fitted separately with that of *INTEGRAL*. The only very marginal effect is that the MOS1/MOS2-*INTEGRAL* spectrum provides (in all spectral models presented) a flatter photon index than the one obtained with the pn-*INTEGRAL* spectrum. The flattening of Γ is however less than 10%. Similarly, the values of the spectral parameters in Table 2, do not change if we use only the *XMM-Newton* data. Furthermore, even the range of uncertainty of these parameters does not change significantly. In fact, the statistics in the broadband anal-

ysis is fully dominated by the higher quality of the *XMM-Newton* data.

4 DISCUSSION

In Figure 2 we show the SED of 4C04.42 where non simultaneous data across the electromagnetic spectrum have been taken from NED¹. In FSRQ the two peaked SED is interpreted in the Synchrotron External Compton framework (Ghisellini et al. 1998): the low frequency peak in the IR or FIR is created through the Synchrotron radiation of relativistic electrons moving in a blob, of dimension R , originating in the jet and a magnetic field of few Gauss. The high frequency peak in the hard-X and gamma-rays is believed to be the effect of IC scattering of the same electrons population on a photon field that can be caused (1) by the Synchrotron radiation (SSC) and/or (2) by thermal emission from the accretion disk, BLR and/or dusty torus (EC). Due to the high density of the external photon field, the EC in FSRQ dominates over the SSC. The secondary effect on the SED derived from EC in the molecular torus, distant on the scale of pc from the central black hole, is not considered here. A model that well reproduce the SED² is also included in Figure 2. The simplest hypothesis is that the emitting region is a blob of radius R moving with a bulk velocity of βc (where $\beta = \sqrt{\Gamma^2 - 1}/\Gamma$, and Γ is the Lorentz factor), in a magnetic field with intensity of 2 Gauss. We assume an observing angle of $\theta \sim 1/\Gamma$ implying a Doppler factor $\delta = \Gamma$. The SSC+EC components are plotted separately in Figure 2 with solid and dashed lines respectively. The disk contribution (dotted line) is shown as

¹ NRAO Extragalactic Database; <http://nedwww.ipac.caltech.edu/index.html>
² SSC code from http://www.asdc.asi.it/ssc_at/. The model was used in e.g. Massaro et al. (2006) and De Rosa et al. (2005)

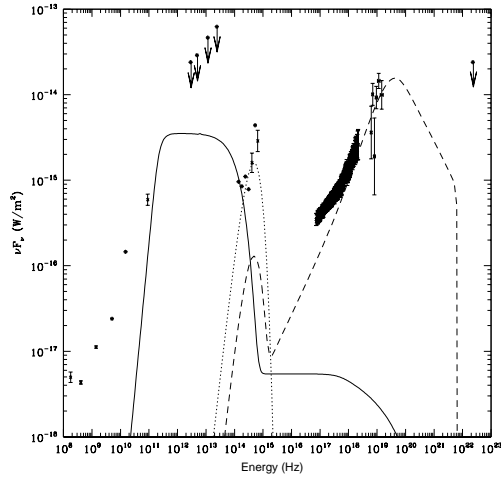


Figure 2. Spectral Energy Distribution from radio up to soft gamma-ray frequencies. Data are from literature taken by NED

a thermal component with temperature of $kT_{BB,z} = 1$ eV in the quasar rest frame. No other additional component, such as reflection from the disk, has been included in the model. The dimension of the emitting blob, the magnetic field, the electron energy distribution, and the Lorentz factor are the only parameters required to evaluate the SSC component in the SED. We assume that the electrons in the blob are well described by a power-law, $N(\gamma) = N \gamma^{-p} \text{ cm}^{-3}$, in the range γ_{min} and γ_{max} , and we do not take into account radiative cooling of the electrons. The input parameters for our model are reported in the Table 3. We stress that our model for the whole SED is not a true “fit”. In view of the not simultaneous data set, we just attempt to extract some physical parameters from the data, with the main goal to obtain average properties of the source. In particular the EC component did allow us to constrain γ_{max} , and p . The EC component due to the BLR photon field is determined by the BLR energy density U_{BLR} . We fixed the disk luminosity at the level of the optical-UV emission (at 10^{15} Hz in the quasar rest frame) observed in the source SED. The BLR luminosity is estimated assuming that that region reprocesses a fraction of the disk luminosity that is ~ 0.1 (Maraschi & Tavecchio 2003). The energy density in the observer frame is given by $U_{BLR}^{oss} = L_{BLR} / 4\pi c R_{BLR}^2$, so that the contribution of the IC emission to the SED is $P_{EC} = 4/3 \sigma_T c \delta^4 \int_{\gamma_{min}}^{\gamma_{max}} N(\gamma) \gamma^2 U_{BLR}^{oss} \Gamma^2 d\gamma = 8 \times 10^{-2} R_{BLR,17}^{-2} \text{ erg cm}^{-3} \text{ s}^{-1}$, where $R_{BLR,17}$ is the BLR extension in units of 10^{17} cm. R_{BLR} is measured in very few AGN through reverberation mapping (Kaspi et al. 2005), where a relation between R_{BLR} and $\lambda L_{\lambda}(5100 \text{ \AA})$ is assumed. Taking $\lambda L_{\lambda}(5100 \text{ \AA})$ from the SED, we have $R_{BLR} = 5 \times 10^{17}$ cm. In the emitting volume given by $V = 4/3 \pi R^3$, we would then expect $L_{EC} = 3 \times 10^{47} \text{ erg s}^{-1}$, in agreement with the value reported in the SED.

Figure 2 clearly shows evidence that the SSC+EC model does not well fit the whole SED. In particular an excess, of about of a factor of three with respect to the EC component, is visible around 2 keV. This soft X-ray excess could be due to bulk Compton of a “cold” shell of plasma moving in the jet and interacting with the external BLR photon field (Celotti et al. 2007). The luminosities of the Bulk and External Compton components, L_{BC} and L_{EC} , are determined by the relative normalizations of the number densities of the cold and relativistic electrons. The number of cold electrons is usually difficult to verify since low energy electrons emit syn-

Table 3. SED model parameters for 4C04.42

¹ B (Gauss)	² R (cm)	³ δ ($=\Gamma$)	⁴ N (cm^{-3})	⁵ $\gamma_{min}/\gamma_{max}$	⁶ p	⁷ L_{BLR} (erg s^{-1})	⁸ R_{BLR} (10^{17} cm)
2	3×10^{16}	20	10^4	1/1000	3	2×10^{45}	5

¹Magnetic field; ²Dimension of the emitting blob; ³Doppler factor assumed to be equal to the bulk Lorentz factor; ⁴number density of the electrons; ⁵minimum/maximum electron Lorentz factor; ⁶electron spectral index; ⁷observed BLR Luminosity; ⁸BLR extension.

chrotron light in the self-absorbed range, and SSC radiation at low frequencies, where the flux is dominated by the Synchrotron emission of electrons of higher energies. The only way to observe the bulk Compton component in the SED is when it dominates the non thermal continuum in the soft X-ray energy range, and this will happen when the competitive processes, like SSC, are negligible in this band. However, here we do not try to fit this excess with a bulk Compton component, we just stress that with $\Gamma=20$, as assumed in our model, we expect to detect the peak of such component at the frequency of $\nu_{BC} = \Gamma^2 \nu_{BLR} / (1+z) \sim 1$ keV, i.e. where the excess is observed. In addition, if the excess is interpreted as due to bulk motion then $L_{BC} = 4/3 \sigma_T c \delta^4 U_{BLR}^{oss} \Gamma^2 N_c \sim 10^{46} N_c / N$, where N_c is the number of cold electrons in the blob. With the value obtained in Sect. 3, $L_{BC} \sim 10^{45} \text{ erg s}^{-1}$, we estimate the ratio N_c/N to be ~ 0.1 . Very recently the bulk Compton process has been proposed as a means to explain the steepening of the spectrum in the case of quasars PKS 1510-089 at $z=0.361$ (Kataoka et al. 2007), 0723-679 at $z=0.847$, 1136-135 at $z=0.554$, and 1150-497 at $z=0.334$ (Sambruna et al. 2006). The bulk Compton process has been also proposed to explain the observed flattening in the powerful blazar BG B1428+4217, at $z=4.72$ (Celotti et al. 2007). In this source the soft X-ray behaviour was previously attributed to warm absorption intrinsic to the source (Fabian et al. 1998, 2001; Yuan et al. 2006). We also stress here that flattening of the spectral emission has been observed in high- z quasars up to $z=4.4$, while the softening has been observed in very few sources, and all are at redshifts below 1 (see Table 4).

Alternative models to bulk Comptonization can be taken into account: (a) an increasing contribution of the SSC component in the energy band between the Synchrotron and EC peaks, as already proposed by Kataoka et al. (2007). However the SED associated with the model in Figure 2 makes this hypothesis unlikely in the case of 4C04.42; (b) the emission originating in the central region of the accretion flow (Done & Nayakshin 2007), as observed in several non-blazar objects; (c) the Synchrotron peak placed in the X-ray band and not at UV frequencies, as observed in some FSRQ (Padovani et al. 2003; Giommi et al. 2007). However, this does not seem to be the case for 4C04.42, in fact, the SED indicates that this peak is in the IR range; (d) the disk emission, assuming that it was composed by a black body from optical to soft X-ray (like in b), plus a flat spectrum reproducing the reflection component at harder X-ray, as proposed by Sambruna et al. (2006) to resolve the excess of soft X-ray emission in three powerful radio loud quasars, 1136-135, 1150-497, 0723-679; (e) Tavecchio & Ghisellini (2008), have recently demonstrated that the EC radiation, computed taking into account a realistic spectrum for the external radiation originated in the BLR (calculated with the photoionization code CLOUDY, Ferland et al. (1998)), shows evidence of a steepening below 1 keV, that does not appear when the EC radiation is computed using a simple black body parameterization for the BLR emission.

Important physical quantities can be derived by a comparison

Table 4. Comparison between the sources that show the excess emission below 2 keV.

Source	z	R _{BLR} (10 ¹⁷ cm)	L _{disk} (10 ⁴⁵ erg s ⁻¹)	*P _{jet} (10 ⁴⁵ erg s ⁻¹)
4C04.42	0.965	5	20	300
⁽¹⁾ 0723+679	0.847	2	10	350
⁽¹⁾ 1136-135	0.554	5.2	5	73
⁽¹⁾ 1150-497	0.334	2.6	3	76
⁽²⁾ 1510-089	0.361	5	4	500

⁽¹⁾ Sambruna et al. (2006); ⁽²⁾ Maraschi & Tavecchio (2003); Kataoka et al. (2007). * calculated for $n_e = n_p$. See text for details.

between the power carried by the jet P_{jet} , and the disk luminosity L_{disk} . Under the assumption of one proton per emitting electron in the jet composition we can estimate the jet kinetic power $P_{jet} = \pi R^2 \beta \Gamma^2 c U$ for 4C04.42, where $U = U_B + U_e + U_p$ is the total energy in the jet rest frame due to magnetic field, electron and protons: $U_e + U_p = n_e m_e c^2 [\langle \gamma \rangle + n_p/n_e (m_p/m_e)]$, with $n_e = \int_{\gamma_{min}}^{\gamma_{max}} N(\gamma) d\gamma$ and $\langle \gamma \rangle$ the average Lorentz factor of the electrons. In Table 4 we provide the values of L_{disk} and P_{jet} for "similar" sources, i.e. those showing an excess at low energies. For 4C04.42, using the model we employed to reproduce the SED and $\gamma_{min} = 1$, we obtain $L_{disk}/P_{jet} \sim 0.1$ which is in very good agreement with the other cases in where this ratio was evaluated with good accuracy (Maraschi & Tavecchio 2003; Sambruna et al. 2006). In the plane L_{disk} vs P_{jet} , 4C04.42 lies in the region of high-luminosity blazars, following the trend observed in other similar sources. This, in turn, implies that a large fraction of the accretion power is converted in bulk kinetic energy of the jet (Maraschi & Tavecchio 2003; Celotti & Ghisellini 2008). We stress that increasing γ_{min} to 10 P_{jet} is augmented by a factor of 10, leaving unchanged our findings.

Finally, we note that the combined broadband *XMM-Newton* and *INTEGRAL* spectral analysis gives us a harder spectral index than typically observed in the radio loud QSOs (Reeves & Turner 2000; Piconcelli et al. 2005). This evidence suggests that this source could be a member of the small subclass of "MeV blazars" (Bloemen et al. 1995; Tavecchio et al. 2000). Future observation in the gamma-ray band with *GLAST* and *AGILE* will be able to address this issue.

5 CONCLUSIONS

We have presented the (non simultaneous) broadband spectral analysis of the powerful quasar 4C04.42 at $z=0.965$ observed by *XMM-Newton* and *INTEGRAL*. Archival data from *NED* allowed us to build the Spectral Energy Distribution and to study possible emitting scenarios in the framework of the SSC+EC models. Our main results are:

- The 2–200 keV spectrum is best reproduced by a power-law model, with photon index ~ 1.2 , i.e. flatter than observed in radio loud QSOs.
- The spectrum below 2 keV (observer frame) clearly shows evidence for a steepening, and the broadband data can be described either with a power-law plus a thermal component with $kT_{BB} = 0.2$ keV or by a broken power-law with $E_{break} = 2$ keV and $\Delta\Gamma = 0.4$. Both models are equally statistically acceptable.
- The doubled peaked SED built with non simultaneous data from radio up to gamma-ray, has been interpreted within a scenario that invokes a blob of relativistic electrons emitting Synchrotron ra-

diation moving in a magnetic field of a few Gauss, plus IC radiation in the photon field of the BLR.

- The excess found in the soft X-ray, as well as the flat spectral shape in hard X-ray, strongly suggests the presence of a population of cold electrons able to produce a bulk Compton feature at ~ 1 keV through IC with the photon field of the BLR.
- The ratio $L_{disk}/P_{jet} \sim 0.1$ between the disk luminosity and the power carried by the jet, implies that a large fraction of the accretion power is converted in bulk kinetic energy of the jet.

This program is funded by Italian Space Agency grant via contracts I/008/07/0 and I/023/05/0. We thank the referee for constructive suggestions.

REFERENCES

- Bassani, L., Landi, R., Malizia, A., et al. 2007, *ApJ*, 669, L1
 Bird, A., Malizia, A., Bazzano, A., et al. 2007, *ApJS*, 170, 175
 Bloemen, H., et al. 1995, *A&A*, 293, L1
 Celotti, A., Ghisellini, G., Fabian, A.C. 2007, *MNRAS*, 375,
 Celotti, A. & Ghisellini, G. 2008, *MNRAS*, 385, 283
 De Rosa, A., Piro, L., Tramacere, A., et al. 2005, *A&A*, 438, 121
 Dermer, C. D., & Schlickeiser, R. 1993, *ApJ*, 416, 458
 Done, C. & Nayakshin, S. 2007, *MNRAS*, 377, L59
 Elvis, M., Wilkes, B. J., McDowell, J. C., et al. 1994, *ApJS*, 95, 1
 Fabian, A. C.; Iwasawa, K.; McMahon, R. G.; et al. 1998, *MNRAS*, 295L, 25
 Fabian, A. C., Celotti, A., Iwasawa, K., et al. 2001, *MNRAS*, 323, 373
 Ferland G. J., Korista K. T., Verner D. A., et al. 1998, *PASP*, 110, 761
 Fiore, F., Elvis, M., Giommi, P., Padovani, P. 1998, *ApJ*, 492, 79
 Fossati, G., Maraschi, L., Celotti, A., Comastri, A., Ghisellini, G. 1998, *MNRAS*, 299, 433
 Ghisellini, G., Celotti, A., Fossati, G., Maraschi, L., Comastri, A. 1998, *MNRAS*, 301, 451
 Giommi, P., Massaro, E., Padovani, P., et al. 2007, *A&A*, 468, 97
 Magdziarz & Zdziarski 1995, *MNRAS*, 273, 837
 Maraschi, L. & Tavecchio, F. 2003, *ApJ*, 593, 667
 Maraschi, L., Ghisellini, G., Celotti, A. 1992, *ApJ*, 397, L5
 Masaro, E., Tramacere, A., Perri, et al., 2006, *A&A*, 448, 861
 Kataoka, J., Madejski, G., Sikora, M., et al. 2008, *ApJ*, 672, 787
 Kaspi, S.; Maos, D; Netzer, H., et al. 2005, *ApJ*, 629, 61
 Kellermann, K. I., Sramek, R., Schmidt, et al. 1989, *AJ*, 98, 1195
 Kirsch, M. G., Briel, U. G., Burrows, D., et al. 2005, *SPiE*, 5898, 22
 Padovani, P., Perlman, E.S., Landt, H., Giommi, P., Perri, M. 2005 *ApJ*, 588, 128
 Page, K. L.; Reeves, J. N.; O'Brien, P. T.; Turner, M. J. L. 2005, *MNRAS*, 364, 195
 Piconcelli, E., Jimenez-Bailin, E., Guainazzi, M., et al. 2005, *A&A*, 432, 15
 Reeves, J. N., & Turner, M. J. L. 2000, *MNRAS*, 316, 234
 Sambruna, R.M, Gliozzi, M., Tavecchio, F., Maraschi, L., Foschini, L. 2006, *ApJ*, 2006, 652, 146
 Sambruna, R. M., Reeves, J. N., Braitto, V. 2007, *ApJ*, 665, 1030
 Tavecchio, F.; Maraschi, L.; Ghisellini, G.; et al., 2000, *ApJ*, 543, 535T
 Tavecchio F. & Ghisellini G. 2008, *MNRAS*, 386, 945
 Ubertini P., Lebrun F., Di Cocco G. et al. 2003, *A&A* 411, 131
 Yuan W., Fabian A.C., Worsley M.A., McMahon R., 2006, *MNRAS*, 368, 985
 Wagner, S. J. et al. 1995, *A&A*, 298, 688